A Direct Data-Driven Control Design for Autonomous Bicycles

Niklas Persson, Mojtaba Kaheni, Alessandro V. Papadopoulos

Abstract— In this work, we address the problem of balancing an autonomous bicycle using direct data-driven control. Firstly, we demonstrate that a direct implementation of data-driven approaches may not guarantee reliable performance, and is highly dependent on how the parameters are selected. To address this issue, we make the reasonable assumption that we have access to some inaccurate information about the system. We use this inaccurate information to design a feedback linearization, based on a simplified point mass model of the bicycle, which does not accurately represent the dynamics of the system. Next, we suggest an inner and outer-loop control strategy. In the inner loop, we implement the aforementioned feedback linearization controller. Subsequently, in the outer loop, we consider the combination of the autonomous bicycle and the feedback controller as a black box, and we design a direct data-driven controller from acquired data. We use a SolidWorks model of a real autonomous bicycle to evaluate the performance of our proposed control approach and to compare it with the direct data-driven controller design derived from acquired data of the bicycle without feedback linearization. The results show that our proposed strategy significantly improves the performance and makes the data-driven control approach more reliable across a broader range of parameter choices compared to a data-driven controller designed based on data from the system without feedback linearization. Finally, we show that introducing an additional integral-like state further enhances the system's performance.

I. INTRODUCTION

The seminal study by Willems et al. [1] revealed a paradigm-shifting concept that has immense potential for revolutionizing control system design. The study demonstrated that a finite set of system trajectories, generated through persistently exciting input, has the capability to represent the complete behavior of a controllable linear system. This finding implies that it is possible to describe controllable time-invariant linear systems solely based on finite historical data, eliminating the need for traditional state-space or transfer function representations. Such a breakthrough has sparked great interest within the control system community, as it offers a promising avenue to streamline control system design by potentially circumventing the costly and time-consuming step of system identification or complex first principle modeling. For instance, [2]–[4] propose predictive data-driven approaches, while [5]–[7] focus on optimal data-driven control methods and [8]–[10] present robust and nonlinear control design.

However, the Fundamental Lemma mentioned in [1], which serves as the basis for data-driven approaches, only
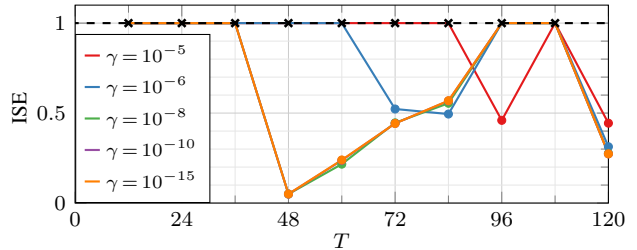

Fig. 1. Integrated squared error (ISE) for an autonomous bicycle tracking a reference lean angle using the DPT controller in simulations with varying parameters. ISE values above 1 are considered unstable and are truncated.

applies to linear systems, while, in practical scenarios, most systems exhibit inherent nonlinearity. Nonlinear data-driven control approaches, introduced up to date, rely on techniques such as linearization [8], [9] or Koopman operators shifting [10], [11]. As a result, the performance of these approaches in practical implementations relies on the accuracy of the linear representation of the nonlinear system.

The case study in this article is an autonomous bicycle. Bicycle dynamics are nonlinear and they exhibit an unstable behavior at low velocities, making it a good illustration of many interesting issues in control design. Various model-based methods have been proposed for balancing an autonomous bicycle, including Sliding Mode Controller (SMC) [12], state feedback controller [13], feedback linearization controller [14], and by combining feedback linearization with LQR and LQI controllers [15], to name a few. In this paper, we investigate how to design a data-driven control approach for balancing a bicycle.

Fig. 1 shows the results obtained by directly applying to the bicycle the data-driven control method for nonlinear systems proposed by De Persis and Tesi [8], referred to as DPT[1] throughout this paper. The controller aims to track a reference lean angle by actuating the steering velocity. The figure shows the Integrated Squared Error (ISE)[2] between the reference and the measured lean angle, as a function of the number of samples, T, used to design the DPT controller. Moreover, the figure shows how the results change as a function of the design parameter γ required for the DPT controller. This design parameter defines the entity of the allowable disturbance, which includes the entity of the system's disturbance and of the mismatch between the nonlinear and linearized system—more details in [8]. The historical input and output data were sampled at a rate of

The authors are affiliated with Mälardalen University, Västerås, Sweden. e-mail: `Firstname.Surname@mdu.se`.

[1]The name comes from the initial of the authors of [8].

[2]Note that in the figure the ISE is clamped to 1 and marked with ✗ when the resulting design is unstable.

100Hz and were obtained by exciting the system input with $u(t) = \frac{36}{\pi}\cos((9-0.4t)t)$ deg/s while the bicycle was riding at a constant velocity of 8km/h.

As can be observed from the initial results depicted in Fig. 1, the performance of the controller depends in a nontrivial way on the sampling size T, and the parameter γ, and it seems difficult to draw any conclusions on how these parameters should be chosen for reliable performance. However, in most practical systems, valuable information about some of the system's dynamics or parameters is available, which could be exploited in the control design. This information might not be sufficiently precise or reliable for designing a controller based solely on it, but it can still be precise enough to mitigate the nonlinear behaviors of a practical system and make the adoption of data-driven approaches smoother.

A. Statement of Contributions

The main contributions of this article are as follows:

- We apply the DPT control for nonlinear systems introduced in [8] to an accurately mechanically modeled autonomous bicycle designed in *SolidWorks*.
- We demonstrate that the minimum number of acquired samples required to design data-driven controllers, as determined in idealized studies, may not be sufficient in practical implementations when dealing with nonlinear unstable systems.
- We enhance the performance of data-driven control for nonlinear systems by incorporating prior information about the system and adding an inaccurate feedback linearization controller to the control design.
- We show that introducing an additional integral-like state can further enhance the system's performance.

B. Organization

The rest of the paper is structured as follows, first, in Section II the control design and fundamental concepts of data-driven control are presented. The control setting and the simulation setup are discussed in Section III followed by the results in Section IV. Finally, concluding remarks and future work are given in Section V.

C. Notation

Throughout this paper, $\mathbb{Z}$, $\mathbb{N}$, and $\mathbb{R}$ represent the sets of integers, positive integers, and real numbers, respectively. Unless clearly specified otherwise, scalars are denoted as x, while $\mathbf{x}$, $\boldsymbol{x}$, and $\mathbf{X}$ denote a (column) vector, a signal, and a matrix, respectively. Given a signal $\boldsymbol{s} : \mathbb{Z} \to \mathbb{R}^d$, of size d, we denote the trimmed $\boldsymbol{s}$ within the time interval $[k, k+T]$, where $T \in \mathbb{N}$ and $k \in \mathbb{Z}$, by $\boldsymbol{s}_{\{k:k+T\}}$, i.e.

$$\boldsymbol{s}_{\{k:k+T\}} \triangleq \{\mathbf{s}(k), \ldots, \mathbf{s}(k+T)\}.$$

Furthermore, we denote the matrix that contains T successive samples of $\boldsymbol{s}$ starts from k by $\mathbf{S}_{[k,T]}$, i.e.

$$\mathbf{S}_{[k,T]} \triangleq \begin{bmatrix} \mathbf{s}(k), & \ldots, & \mathbf{s}(T+k-1) \end{bmatrix}.$$

Furthermore, $\mathrm{diag}([x_1, \ldots, x_n])$ denotes a diagonal matrix with the elements $x_1, \ldots, x_n$ on its diagonal. Finally, $\mathrm{tr}(\mathbf{X})$, $\mathrm{rank}(\mathbf{X})$, and $\mathbf{X}'$ denote the trace, rank, and transpose of matrix $\mathbf{X}$, respectively.

II. DIRECT DATA-DRIVEN CONTROL

This section introduces some preliminaries for designing controllers based solely on the historical input and output data of a system. Next, the DPT controller [8] is presented.

Consider a discrete linear time-invariant system

$$\mathbf{x}(k+1) = \mathbf{A}\mathbf{x}(k) + \mathbf{B}\mathbf{u}(k), \quad k \in \mathbb{N}, \tag{1}$$

where $\mathbf{x} \in \mathbb{R}^n$ and $\mathbf{u} \in \mathbb{R}^m$ represent the state and input vectors, respectively. We assume that T historical samples of $\mathbf{u}$ are accessible, where $T \in \mathbb{N}$. In other words, the signal $\boldsymbol{u}_{\{0:T-1\}}$ is known. We recall the fundamental property introduced by Willems et al. [1] that establishes a necessary condition for the T-long historical data of $\mathbf{x}(k)$ and $\mathbf{u}(k)$ to effectively represent the dynamical system described by (1). Let us begin by defining the concept of persistently exciting inputs.

Definition 1 ([1]): The signal $\boldsymbol{u}_{\{0:T-1\}} \in \mathbb{R}^m$ is said to be persistently exciting of order l if

$$\mathcal{U}_0 = \begin{bmatrix} \mathbf{u}(0) & \mathbf{u}(1) & \cdots & \mathbf{u}(T-l) \\ \mathbf{u}(1) & \mathbf{u}(2) & \cdots & \mathbf{u}(T-l+1) \\ \vdots & \vdots & \ddots & \vdots \\ \mathbf{u}(l-1) & \mathbf{u}(l) & \cdots & \mathbf{u}(T-1) \end{bmatrix},$$

has full rank ml. ∎

Definition 1 implies that signal $\boldsymbol{u}$ must be sufficiently long, namely

$$T \geq (m+1)l - 1, \tag{2}$$

to be persistently exciting. The following lemmas play a key role in the data-driven approaches used in this paper.

Lemma 1 ([1]): If the system (1) is controllable and $\boldsymbol{u}_{\{0:T-1\}}$ is persistently exciting of order $n+1$, then

$$\mathrm{rank}(\mathcal{W}_0) = n + m,$$

where

$$\mathcal{W}_0 := \begin{bmatrix} \mathbf{U}_{[0,T]} \\ \mathbf{X}_{[0,T]} \end{bmatrix}.$$

∎

In [8], De Persis and Tesi transformed the state space representation in (1) into a form that exclusively relies on historical data.

Lemma 2 ([8]): If $\boldsymbol{u}_{\{0:T-1\}}$ is persistently exciting, then the system (1) with a state feedback $\mathbf{u} = \mathbf{K}\mathbf{x}$ can be represented by:

$$\mathbf{x}(k+1) = \mathbf{X}_{[1,T]}\mathcal{G}_{\mathbf{K}}\mathbf{x}(k), \tag{3}$$

where $\mathcal{G}_{\mathbf{K}}$ is a $T \times n$ matrix that satisfies

$$\begin{bmatrix} \mathbf{K} \\ \mathbf{I}_n \end{bmatrix} = \mathcal{W}_0 \mathcal{G}_{\mathbf{K}}, \tag{4}$$

and as a result

$$\mathbf{u}(k) = \mathbf{U}_{[0,T]}\mathcal{G}_{\mathbf{K}}\mathbf{x}(k). \tag{5}$$

∎

From (3) we notice that in the closed-loop discrete system (1) under state-feedback control $\mathbf{u} = \mathbf{K}\mathbf{x}$ it holds,

$$\mathbf{A} + \mathbf{B}\mathbf{K} = \mathbf{X}_{[1,T]}\mathcal{G}_{\mathbf{K}}. \tag{6}$$

Thus, one can find an appropriate $\mathcal{G}_{\mathbf{K}}$ so that $\mathbf{X}_{[1,T]}\mathcal{G}_{\mathbf{K}}$ satisfies the classical Lyapunov stability condition. In [8], De Persis and Tesi proved that if $\text{rank}(\mathcal{W}_0) = n + m$, then $\mathbf{K}$ defined by

$$\mathbf{K} = \mathbf{U}_{[0,T]}\mathbf{Q}\left(\mathbf{X}_{[0,T]}\mathbf{Q}\right)^{-1}, \tag{7}$$

asymptotically stabilizes (1) by any matrix $\mathbf{Q}$ that satisfies

$$\begin{bmatrix} \mathbf{X}_{[0,T]}\mathbf{Q} & \mathbf{X}_{[1,T]}\mathbf{Q} \\ \mathbf{Q}'\mathbf{X}'_{[1,T]} & \mathbf{X}_{[0,T]}\mathbf{Q} \end{bmatrix} \succ 0. \tag{8}$$

A. DPT Control for Nonlinear Systems

Based on the results of the data-driven state-feedback controller in (7), the authors in [8] investigated the conditions under which the linearization around the equilibrium point can be implemented to drive a data-driven approach for controlling smooth nonlinear systems. Consider a nonlinear system defined by

$$\mathbf{x}(k+1) = f(\mathbf{x}(k), \mathbf{u}(k)), \tag{9}$$

suppose that f is continuous and differentiable and $(\bar{\mathbf{x}}, \bar{\mathbf{u}})$, which serves as the target for moving the system's states towards, is known. By linearization around this equilibrium point, one can rewrite (9) as

$$\Delta\mathbf{x}(k+1) = \mathbf{A}\Delta\mathbf{x}(k) + \mathbf{B}\Delta\mathbf{u}(k) + \mathbf{d}(k), \tag{10}$$

where $\Delta\mathbf{x}(k) := \mathbf{x}(k) - \bar{\mathbf{x}}$, $\Delta\mathbf{u}(k) := \mathbf{u}(k) - \bar{\mathbf{u}}$ and

$$\mathbf{A} := \left.\frac{\partial f}{\partial\mathbf{x}}\right|_{(\mathbf{x},\mathbf{u})=(\bar{\mathbf{x}},\bar{\mathbf{u}})}, \quad \mathbf{B} := \left.\frac{\partial f}{\partial\mathbf{u}}\right|_{(\mathbf{x},\mathbf{u})=(\bar{\mathbf{x}},\bar{\mathbf{u}})}. \tag{11}$$

In [8], it is proved that if the matrices

$$\begin{bmatrix} \Delta\mathbf{U}_{[0,T]} \\ \Delta\mathbf{X}_{[0,T]} \end{bmatrix}, \quad \Delta\mathbf{X}_{[1,T]},$$

have full rank and $\mathbf{d}(k)$ is upper bounded such that there exists $\gamma > 0$ that satisfies

$$\mathbf{D}_{[0,T]}\mathbf{D}'_{[0,T]} \preceq \gamma\Delta\mathbf{X}_{[1,T]}\Delta\mathbf{X}'_{[1,T]}, \tag{12}$$

then the state-feedback $\mathbf{K} = \Delta\mathbf{U}_{[0,T]}\mathbf{Q}(\Delta\mathbf{X}_{[0,T]}\mathbf{Q})^{-1}$, which has similar shape to (7), locally stabilizes the system by any $(\mathbf{Q}, \mu)$ that satisfies

$$\begin{bmatrix} \Delta\mathbf{X}_{[0,T]}\mathbf{Q} - \mu\Delta\mathbf{X}_{[1,T]}\Delta\mathbf{X}'_{[1,T]} & \Delta\mathbf{X}_{[1,T]}\mathbf{Q} \\ \mathbf{Q}'\Delta\mathbf{X}'_{[1,T]} & \Delta\mathbf{X}_{[0,T]}\mathbf{Q} \end{bmatrix} \succ 0,$$

$$\begin{bmatrix} \mathbf{I}_T & \mathbf{Q} \\ \mathbf{Q}' & \Delta\mathbf{X}_{[0,T]}\mathbf{Q} \end{bmatrix} \succ 0, \quad \frac{\mu^2}{(4+2\mu)} > \gamma. \tag{13}$$

Remark 1: In DPT, it is assumed that the exact dynamical system model is unknown. Consequently, the precise value of $\mathbf{D}_{[0,T]}$ in (12) remains unknown. Therefore, determining the lower bound of γ that satisfies (13) through mathematical means is not feasible. As a result, the tuning of γ in DPT must be conducted experimentally.

III. AUTONOMOUS BICYCLE CONTROL DESIGN

The results depicted in Fig. 1 show that the DPT controller in (13) may not always deliver reliable performance. Under certain parameter combinations, the system becomes unstable. Furthermore, the inherent instability of a bicycle at low velocities complicates the task of sampling input and output data. For example, when the bicycle leans to the left and is steered to the right, it quickly falls over. In contrast, steering to the left eventually stabilizes it and brings it back to an upright position. These characteristics render some input signals infeasible for acquiring data.

In this section, we make a reasonable assumption that some imprecise and simplified information about the system is available. We address both of the aforementioned challenges by implementing output feedback linearization, using the available inaccurate information to reduce the nonlinear behavior of the system and push it toward linearity. Subsequently, to improve the closed-loop performance of the system compared to relying solely on feedback linearization or data-driven control, we design a data-driven controller for the system composed of the autonomous bicycle and the feedback linearization. Given that the nonlinear data-driven control approaches introduced up to date rely on techniques such as linearization [8], [9] or Koopman operators shifting [10], [11], this modification can offer performance improvements by reducing the nonlinearities of the system. Additionally, this section provides details on the multibody simulation of the bicycle and an explanation of how the data was collected.

A. Control Design

Consider the following point mass model of a bicycle [16]:

$$\begin{aligned} h^2\ddot{\varphi}(t)m = {} & gm\left(h\sin\left(\varphi(t)\right) + \frac{ca}{b}\sin(\lambda)\sigma(t)\cos\left(\varphi(t)\right)\right) - \\ & \left(1 - \frac{h}{b}\sigma(t)\sin\left(\varphi(t)\right)\right)\frac{h}{b}\sigma(t)\cos\left(\varphi(t)\right)v^2(t)m \\ & - \frac{ahm}{b}\cos\left(\varphi(t)\right)\left(\sigma(t)\dot{v}(t) - v(t)\omega_\sigma(t)\right), \end{aligned} \tag{14}$$

where h and a are the vertical and horizontal distances between the center of gravity and the contact point between the rear wheel and the ground, denoted P_1 in Fig. 2. Gravity, wheelbase, mass, trail, and head angle are denoted g, b, m, c, and λ respectively. The curvature of the bicycle is represented by

$$\sigma(t) = \frac{\tan(\delta(t))\sin(\lambda)}{\cos(\varphi(t))}, \tag{15}$$

where δ and φ represent the steering and lean angles respectively, and $\omega_\sigma(t) = \dot{\sigma}(t) \approx \dot{\delta}(t)\sin(\lambda)$. By assuming a constant forward velocity ($\dot{v} = 0$) and a vertical steering axis ($\lambda = 90, c = 0$), (14) can be simplified as:

$$\begin{aligned} \ddot{\varphi}(t) = {} & \frac{g}{h}\sin\left(\varphi(t)\right) + \frac{a}{bh}\cos\left(\varphi(t)\right)v\dot{\delta}(t) - \\ & \left(\frac{1}{bh} - \frac{1}{b^2}\tan\left(\delta(t)\right)\tan\left(\varphi(t)\right)\right)\tan\left(\delta(t)\right)v^2, \end{aligned} \tag{16}$$

with $\mathbf{x}(t) = [\varphi(t), \dot{\varphi}(t), \delta(t)]'$ and $u(t) = \dot{\delta}(t)$. Although (16) is not full-state linearizable, it can be partially linearized by output feedback linearization.

Let $y(t) = \varphi(t)$, $\dot{y}(t) = \dot{\varphi}(t)$, and let the desired output and its time derivatives be denoted $y_d(t)$, $\dot{y}_d(t)$, and $\ddot{y}_d(t)$. If we choose $u = \dfrac{1}{p(x)}(w - f(x))$, where

$$
\begin{aligned}
f(x) &= -\left(\frac{1}{bh} - \frac{1}{b^2} \tan\left(x_3\right) \tan\left(x_1\right) \right) \tan\left(x_3\right) v^2, \\
&\quad + \frac{g}{h} \sin\left(x_1\right) \\
p(x) &= \frac{a}{bh} \cos\left(x_1\right) v, \\
w &= \ddot{y}_d(t) + k_1 \left(\dot{y}_d(t) - \dot{y}(t) \right) + k_2 \left(y_d(t) - y(t) \right).
\end{aligned}
\tag{17}
$$

Then, by properly selecting k_1 and k_2, the nonlinearities of the system are partially canceled.

Remark 2: It is worth highlighting that the objective of feedback linearization in (17) is to push the nonlinear dynamics of the system toward linearity. The stability of the overall system will be achieved by the outer loop data-driven controller. Therefore, there is no necessity to investigate the stability of the internal dynamic or to select k_1 and k_2 in a way that stabilizes the observable dynamics. However, choosing $k_1 > 0$ and $k_2 > 0$ to satisfy the Routh–Hurwitz stability criterion of the linearized system makes the sampling phase smoother.

Since (16) does not perfectly represent the actual system, applying (17) results in the presence of nonlinearities in the data sampled from the multibody model of the bicycle. Furthermore, perfect knowledge of the system and all the system's parameters is rarely available in practical applications. Therefore, we consider the mismatches, as listed in Table I, between the parameters used in the multibody model and the control law. Throughout the paper, we choose the feedback gains in (17) to $k_1 = 10$ and $k_2 = 10$. Optimization of these parameters could improve the results, however, it is out of the scope of this paper.

As depicted in Fig. 3, we propose the implementation of feedback linearization, introduced in (17), as the inner control loop responsible for mitigating the nonlinear behavior of the system. We consider our autonomous bicycle and the feedback linearization controller, depicted by the gray rectangle in the figure, as a new black box, for which we aim to design a data-driven controller. During the first T samples,

TABLE I

ACTUAL AND ESTIMATED PARAMETERS OF THE INSTRUMENTED BICYCLE.

Geometric parameters				
Parameter	Symbol	Unit	Real value	Estimated value
CoG w.r.t. P_1 (x)	a	m	0.473	0.550
CoG w.r.t. P_1 (z)	h	m	0.515	0.700
Wheelbase	b	m	1.080	1.200

Fig. 2. Instrumented bicycle.

we position the switch in (a) to enable the transmission of the persistently exciting signal $\boldsymbol{u}_{\{0:T-1\}}$ to the system. Subsequently, we position the switch in (b) and apply the designed DPT state-feedback controller $\mathbf{u}(k) = \mathbf{Kx}(k)$ using (13). The feedback linearization control in the inner loop reduces the nonlinearities of the autonomous bicycle, bringing the overall system closer to linearity. Consequently, we anticipate that data-driven results should fit better, leading to improved outcomes compared to the results presented in Fig. 1.

B. Simulation setup

To evaluate our proposed control setting, we employ a multi-body simulation model of an instrumented bicycle [17]. The instrumented bicycle is initially designed using *Solid-Works* and subsequently imported into Mathworks *Simscape*. Two revolute joints connect the rear wheel and the front wheel to the bicycle's frame and fork, respectively, as depicted by 1 and 2 in Fig. 2. Additionally, a third revolute joint connects the fork to the frame, highlighted as 3 in the figure, and is actuated using the proposed controller.

To model the steering dynamics, including the steering motor, we employ a step response matching procedure [17]. The resulting transfer function, from the input, $\mathbf{u}(t)$, to the steering rate, $\dot{\delta}(t)$, is

$$
H(s) = \frac{100 + s}{100},
\tag{18}
$$

and is incorporated in series with the bicycle model, as illustrated in Fig. 3. The gray rectangle in the figure illustrates the system that is treated as a black box when sampling data between the points $\mathbf{u}(k)$ and $\mathbf{x}(k)$. The switch in the figure represents the setup of the system when we sample data (a) and when the DPT control stabilizes the system in a feedback loop (b). The normal force between the tires and the ground is modeled with a stiffness of 10^6N/m, a damping coefficient of 10^3N/(m/s), and a transition region width of 10^{-4}m. In addition, we utilize a smooth stick-slip method to model the friction between the tires and the ground. This method incorporates static and dynamic friction parameters of 0.9 and 0.75, respectively. The critical velocity, which determines the friction parameter to consider, is set to 10^{-3}m/s.
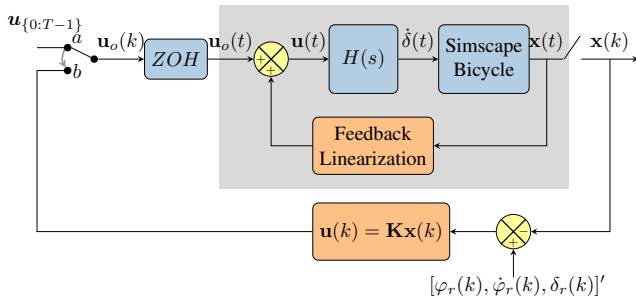
Fig. 3. Block diagram of the control system.

Let $\varphi(k)$ and $\delta(k)$ denote the bicycle lean and steer angles at time step k, respectively. $\mathbf{u}(k)$ represents the control input and is utilized to stabilize the bicycle by steering in the direction of the lean angle. The simulation is initialized with zero steer and lean angle, i.e., $\delta(0) = 0$ and $\varphi(0) = 0$, along with a forward velocity of 8km/h. It is worth noting that this velocity is below the so-called self-stabilization speed of the bicycle [18]. As a result, without proper actuation, the bicycle would inevitably fall over.

C. Data collection

We explore two scenarios, related to the states that we sampling data from in our study,

- *Scenario 1:* $\mathbf{x}(k) = [\varphi_e(k), \dot{\varphi}_e(k), \delta_e(k)]'$,
- *Scenario 2:* $\mathbf{x}(k) = [\varphi_e(k), \dot{\varphi}_e(k), \delta_e(k), \sum_{i=0}^{k} \varphi_e(i)]'$,

where $\varphi_e(k)$, $\dot{\varphi}_e(k)$ and $\delta_e(k)$ denote the difference between the lean angle, lean rate, and steering angle, with the desired values, respectively, i.e. $\varphi_e(k) = \varphi_r(k) - \varphi(k)$. Furthermore, $\sum_{i=0}^{k} \varphi_e(i)$ is the sum of the lean angle error. In the first scenario, as proposed for designing the model-based LQR controller in [17], we assume that the state vector consists of $[\varphi_e(k), \dot{\varphi}_e(k), \delta_e(k)]'$. It is important to note that we implicitly assume the order of the autonomous bicycle system to be 3 in this scenario. The exact order of the system is a crucial parameter, typically assumed to be known in published articles in the field of data-driven control, as authors often start their simulations based on a known mathematical model. However, practical systems generally have more actual states than their simplified mathematical models account for. These neglected states, along with disturbances in (9), which include both nonlinearities and actual system disturbances, can degrade the performance of the control system and lead to steady-state errors. To address this undesired behavior, we introduce an additional state, denoted as $\sum_{i=0}^{k} \varphi_e(i)$, in the second scenario. This approach draws inspiration from linear control theory, where proportional feedback of the integral of the error is commonly employed to compensate for steady-state errors [19].

Data were sampled at a rate of 100Hz from experiments conducted at a constant velocity of 8 km/h. Two datasets were collected, with the first dataset sampled from the unstable system without feedback linearization. In this system, the input signal was a sinusoidal function, represented as $\mathbf{u}_{\{0:T-1\}} = \frac{36}{\pi} \cos((9 - 0.4t)t)$ deg/s. This choice was
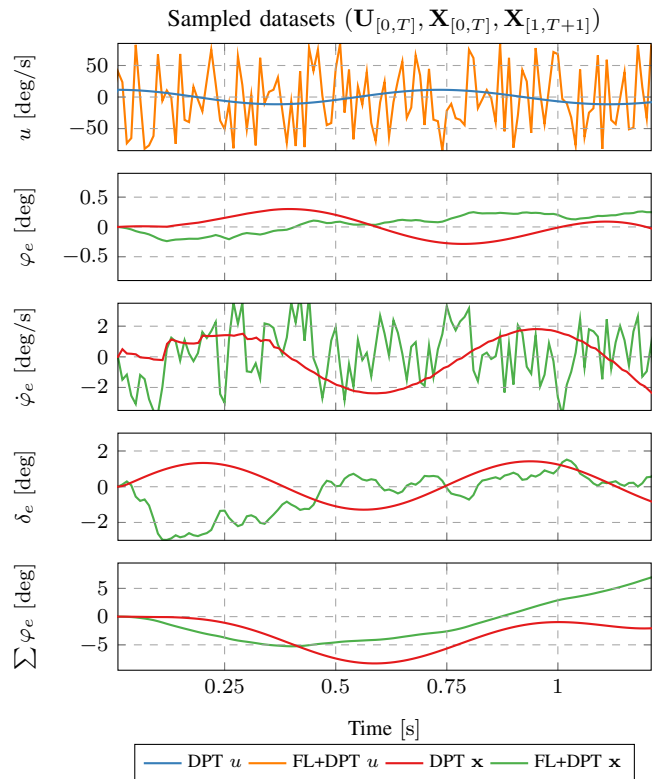

Fig. 4. Collected data from the control signal, $\mathbf{u}$, at the top followed by the four states φ_e, $\dot{\varphi}_e$, δ_e, $\sum \varphi_e$ respectively.

motivated by the highly unstable nature of a bicycle at low velocities, making it necessary to gather sufficient data to capture the primary dynamics of the bicycle.

In the second dataset, when the system is initially stabilized using feedback linearization, the restrictions on the input signal can be neglected. Instead, an input signal $\mathbf{u}_{\{0:T-1\}}$ sampled from a uniform distribution $\mathcal{U}(-1.5, 1.5)$ rad/s is utilized. For both datasets, we considered 120 samples, as shown in Fig. 4, for control design. It is important to note that both of our proposed data collection settings ensure that the input signal remains persistently exciting, satisfying the condition in (2). The dataset from the unstable system was used to design the DPT control, whilst the second dataset, from the stable system, was used to design the Feedback Linearization DPT (FL+DPT) control.

IV. NUMERICAL RESULTS

In the simulation, the bicycle maintains a constant forward velocity of 8 km/h and tracks a reference lean angle. The reference lean angle, represented by a black dashed line in Fig. 5, consists of two sections. The first section features a sinusoidal pattern, $\varphi_r = \frac{36}{\pi} \sin(t)$ deg/s, followed by a section with a constant lean angle of zero degrees. Both $\dot{\varphi}$ and δ track a reference of zero.

To solve (13) for various combinations of γ and T, we employed CVX [20]. In Fig. 5, a comparison is presented between the two different controllers and the two scenar-
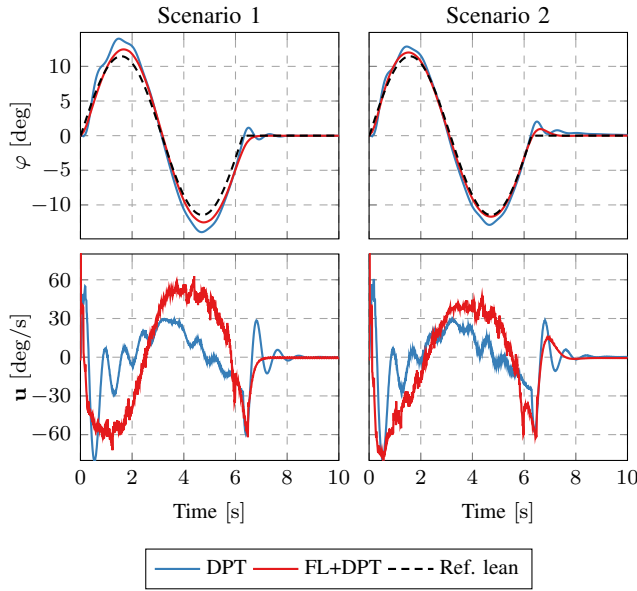
Fig. 5. Tracking comparison of DPT and FL+DPT in Scenario 1 and Scenario 2. The roll angle is presented in the plots at the top of the figure, and the steering velocity input at the bottom of the figure.

ios. The performance displayed in Fig. 5 is based on 120 historical samples from Scenario 1 to design DPT and 120 historical samples from Scenario 2 to design FL+DPT[3]. For both controllers, we used $\gamma = 10^{-15}$. Table II reports the corresponding feedback gain matrices, defined by:

$$\begin{aligned} \text{Scenario 1:} \quad & \mathbf{K} = [k_{\varphi_e}, k_{\dot{\varphi}}, k_{\delta_e}], \\ \text{Scenario 2:} \quad & \mathbf{K} = [k_{\varphi_e}, k_{\dot{\varphi}}, k_{\delta_e}, k_{\sum \varphi_e}]. \end{aligned} \quad (19)$$

TABLE II
RESULTING GAINS FOR THE DIFFERENT CONTROLLERS WITH $\gamma = 10^{-15}$ AND T = 120.

	K			
	k_{φ_e}	$k_{\dot{\varphi}_e}$	k_{δ_e}	$k_{\sum \varphi_e}$
DPT				
Scenario 1	-43.8419	-1.4154	-3.7688	—
Scenario 2	-45.9845	-2.4332	-2.9955	-0.2471
FL+DPT				
Scenario 1	-140.0391	-10.2119	8.2020	—
Scenario 2	-165.1003	-11.6436	9.9205	-4.4944

To investigate the impact of γ in (13) and T, an extensive simulation study was conducted for both Scenarios 1 and 2. The simulations encompassed five distinct values for γ in (13). For each scenario, and each value of γ, 10 different sample sets, $T_1, T_2, \ldots, T_{10}$, was considered where each sample set increased by 12 samples, i.e., $T_1 = 12, T_2 = 24, \ldots, T_{10} = 120$. The comparison of results, illustrated in Fig. 6, focused on evaluating the Integrated Squared Error (ISE) between the lean angle and the reference lean angle,

i.e.

$$\text{ISE}(k) = \sum_{i=0}^{k} (\varphi(i) - \varphi_r(i))^2. \quad (20)$$

ISE values larger than the set threshold of 1, are truncated to 1 and marked with an ✗ in Fig. 6. This indicates that the controller was not able to stabilize the bicycle or that the LMI in (13) were unfeasible, resulting in no feedback gains.
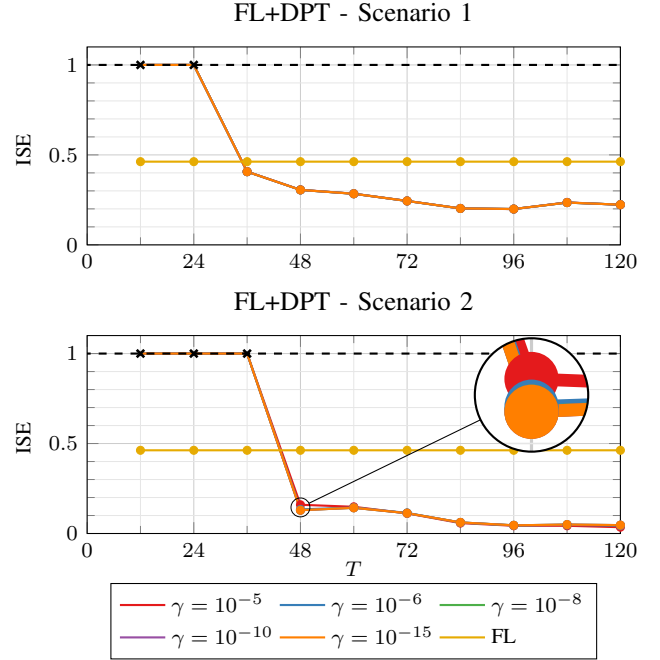

Fig. 6. Performance, in terms of the ISE, by applying FL+DPT. The top plot shows the results from Scenario 1 when three states are considered in the sampling process and the feedback loop. Scenario 2, given in the bottom plot, shows the results when a fourth state, $\sum_{i=0}^{k} \varphi_e(i)$, is added to the control design.

A. Discussion

The simulation results presented in Fig. 5 demonstrate the effectiveness of both DPT and FL+DPT controllers. Remarkably, these controllers, relying solely on 120 samples of input and output data, not only balance an autonomous bicycle but also successfully track a nonzero reference lean angle with small deviations. The effectiveness of the proposed method of adding feedback linearization is clear when comparing the results in Fig. 1 with Fig. 6. By adding feedback linearization, based on a simplified model with errors in the parametric estimation, the performance in terms of the ISE is improved for almost all combinations of γ and T. Moreover, Fig. 6, for $T \geq 48$ the performance variations between different values of γ are very small in both scenarios, thus, increasing the reliability compared to the results in Fig. 1, where the DPT controller was design from data acquired from the unstable system. From Fig. 6 it is also evident that the results from the initially stable system using feedback linearization, highlighted by the yellow line in the figure, are improved by adding DPT for $T \geq 48$. Furthermore, the results in Figs. 5 and 6 clearly show that

by adding a fourth state, $\sum_{i=0}^{k} \varphi_e(i)$, the performance further improves. In practical applications, finding the exact order of a system can be challenging [21]. As a result, in practice, we typically measure or estimate a reduced-dimensional vector of states and implicitly assume that the system's order is limited to them. However, it is clear from the presented results that it can be sensible to modify the number of states.

Moreover, Lemma 1 along with (2) implies that only 7 samples in Scenario 1 and 9 samples in Scenario 2 might be sufficient to obtain a stabilizing controller. However, the outcomes illustrated in Figs. 1 and 6 reveal that designing a data-driven feedback controller based on a limited set of historical samples can potentially compromise the stability of practical systems. As a result, it is advisable to refrain from relying solely on a small subset of historical samples that may not fully capture the nonlinear characteristics and complexities of a system.

V. Conclusion

In this paper, we utilize feedback linearization based on an imprecise and simplified point mass model of a bicycle. The primary objective is to mitigate nonlinearities while simultaneously achieving system stability, which simplifies the process of acquiring input/output data. Subsequently, we regard the bicycle, initially stabilized by feedback linearization, as a new system for which we have limited information. We treat it as a black box, and our goal is to develop a nonlinear direct data-driven controller for its regulation. To evaluate the performance of the approach, numerous simulations are conducted using a realistic Solidworks model of an autonomous bicycle. The results indicate that our proposed method enhances overall outcomes and makes the control approach more reliable across a broader spectrum of parameter choices.

Future research directions include conducting experimental evaluations of the proposed approaches on the instrumented bicycle. Additionally, the results presented in this paper can be extended by exploring the path-tracking capabilities of an autonomous bicycle using data-driven control. Moreover, recognizing the inevitability of the bicycle encountering various working conditions during its operation (e.g., different wind speeds, road conditions, etc.), and exploring dynamical data-driven designs that allow for online updating of the controller are beneficial.

ACKNOWLEDGMENT

References

[1] J. C. Willems, P. Rapisarda, I. Markovsky, and B. L. De Moor, "A note on persistency of excitation," *Systems & Control Letters*, vol. 54, no. 4, pp. 325–329, 2005.

[2] D. Alpago, F. Dörfler, and J. Lygeros, "An extended kalman filter for data-enabled predictive control," *IEEE Control Systems Letters*, vol. 4, no. 4, pp. 994–999, 2020.

[3] J. Coulson, J. Lygeros, and F. Dörfler, "Distributionally robust chance constrained data-enabled predictive control," *IEEE Transactions on Automatic Control*, vol. 67, no. 7, pp. 3289–3304, 2022.

[4] L. Huang, J. Zhen, J. Lygeros, and F. Dörfler, "Robust data-enabled predictive control: Tractable formulations and performance guarantees," *IEEE Transactions on Automatic Control*, vol. 68, no. 5, pp. 3163–3170, 2023.

[5] Z. Yuan and J. Cortés, "Data-driven optimal control of bilinear systems," *IEEE Control Systems Letters*, vol. 6, pp. 2479–2484, 2022.

[6] C. D. Persis and P. Tesi, "On persistency of excitation and formulas for data-driven control," in *Conference on Decision and Control (CDC)*, 2019, pp. 873–878.

[7] G. Baggio, V. Katewa, and F. Pasqualetti, "Data-driven minimum-energy controls for linear systems," *IEEE Control Systems Letters*, vol. 3, no. 3, pp. 589–594, 2019.

[8] C. De Persis and P. Tesi, "Formulas for data-driven control: Stabilization, optimality, and robustness," *IEEE Transactions on Automatic Control*, vol. 65, no. 3, pp. 909–924, 2020.

[9] C. De Persis and P. Tesi, "Low-complexity learning of linear quadratic regulators from noisy data," *Automatica*, vol. 128, p. 109548, 2021.

[10] C. Ren, H. Jiang, C. Li, W. Sun, and S. Ma, "Koopman-operator-based robust data-driven control for wheeled mobile robots," *IEEE/ASME Transactions on Mechatronics*, vol. 28, no. 1, pp. 461–472, 2023.

[11] R. Strässer, J. Berberich, and F. Allgöwer, "Robust data-driven control for nonlinear systems using the koopman operator," in *IFAC World Congress*, Yokohama, Japan, July 2023.

[12] M. Defoort and T. Murakami, "Sliding-mode control scheme for an intelligent bicycle," *IEEE Transactions on Industrial Electronics*, vol. 56, no. 9, pp. 3357–3368, 2009.

[13] C.-F. Huang, Y.-C. Tung, and T.-J. Yeh, "Balancing control of a robot bicycle with uncertain center of gravity," in *International Conference on Robotics and Automation (ICRA)*, 2017, pp. 5858–5863.

[14] N. Getz, "Control of balance for a nonlinear nonholonomic non-minimum phase model of a bicycle," in *Proceedings of 1994 American Control Conference - ACC '94*, vol. 1, 1994, pp. 148–151 vol.1.

[15] A. Owczarkowski, D. Horla, and J. Zietkiewicz, "Introduction of feedback linearization to robust lqr and lqi control – analysis of results from an unmanned bicycle robot with reaction wheel," *Asian Journal of Control*, vol. 21, no. 2, pp. 1028–1040, 2019.

[16] J. Yi, Y. Zhang, and D. Song, "Autonomous motorcycles for agile maneuvers, part i: Dynamic modeling," in *Proceedings of the 48h IEEE Conference on Decision and Control (CDC)*, 2009, pp. 4613–4618.

[17] N. Persson, T. Andersson, A. Fattouh, M. C. Ekström, and A. V. Papadopoulos, "A comparative analysis and design of controllers for autonomous bicycles," in *European Control Conference (ECC)*, 2021, pp. 1570–1576.

[18] J. D. Kooijman, A. L. Schwab, and J. P. Meijaard, "Experimental validation of a model of an uncontrolled bicycle," *Multibody System Dynamics*, vol. 19, pp. 115–132, 2008.

[19] G. F. Franklin, J. D. Powell, and A. Emami-Naeini, *Feedback Control of Dynamic Systems*, 7th ed. Boston, MA: Pearson, 2015.

[20] M. Grant and S. Boyd, "CVX: Matlab software for disciplined convex programming, version 2.1," http://cvxr.com/cvx, Mar. 2014.

[21] D. Liu, Y. Bao, and H. Li, "Machine learning-based stochastic subspace identification method for structural modal parameters," *Engineering Structures*, vol. 274, p. 115178, 2023.